

Ferromagnetic Behavior above Room Temperature of Fe-Ion-Implanted ZnO

Y. Y. SONG, K. S. PARK, D. V. SON, S. C. YU and H. J. KANG*

*BK21 Physics Program and Department of Physics,
Chungbuk National University, Cheongju 361-763*

S. W. SHIN and C. N. WHANG

Department of Physics, Yonsei University, Seoul 120-749

J. H. LEE

Department of Materials Science and Engineering, Korea University, Seoul 136-701

J. H. SONG

Korea Institute of Science and Technology, Seoul 136-761

K. W. LEE

Korea Research Institute of Standards and Science, Daejeon 305-340

(Received 6 September 2006, in final form 13 April 2007)

Zinc-oxide (0001) single crystals with a 0.5 mm thickness were prepared, and then 80 keV Fe ions with a dose of 3×10^{16} ions/cm² were implanted into the ZnO single crystals at 350 °C. The implanted samples were post-annealed at 700, 800 and 900 °C by rapid thermal annealing in an N₂ atmosphere for 5 min to remove the ion-implantation damage. The structure and the magnetic properties of Fe-ion-implanted ZnO were investigated by using X-ray diffraction and a superconducting quantum interference device magnetometer. The carrier transport properties were measured in the range from 5 K to 300 K. The X-ray diffraction results showed an island peak near 37 °C, which was identified as ZnO₂. The magnetization curve showed hysteresis loops at 5 K in the samples annealed at 700 and 800 °C, showing ferromagnetism. Hysteresis loops were observed at 300 K in the samples annealed at 700 °C. The temperature dependence of the magnetization was taken in field cooling (FC) and zero field cooling (ZFC) in the samples annealed at 700 °C. The difference magnetization (ΔM) between the FC and the ZFC magnetizations did not converge to a zero value even at 340 K, showing ferromagnetism above room temperature. The magnetoresistance (MR) curve showed negative curvature up to 150 K which could be explained with the delocalized *d* state of ZnO implanted with Fe ions.

PACS numbers: 75.50.Pp

Keywords: Ferromagnetism, Fe-implanted ZnO

I. INTRODUCTION

Diluted magnetic semiconductors (DMS) have attracted great attention as semiconductor spin transfer electronic (spintronic) devices focused on the manipulation of spin, rather than only electrical charge [1-4]. The first materials known to be DMS were II-VI and III-V semiconductors diluted with transition metal ions like Mn⁺², Cr⁺², Fe⁺², Co⁺², *etc.* [5] because such +2

magnetic ions are easily incorporated into the host II-VI crystals. As a typical material of II-VI semiconductors, ZnO has emerged as an attractive material for DMS because of its wide band gap of 3.37 eV at room temperature [6]. According to Sato *et al.* [7], it shows ferromagnetism above room temperature. Ion implantation can be used to dope transition materials into ZnO semiconductors and it has been quite effective in surveying possible DMS systems with various transition metals [8, 9].

In this work, Fe-ion-implanted ZnO was prepared and post-annealed at various temperatures. The difference

*E-mail: hjkang@chungbuk.ac.kr; Fax: +82-43-274-7811

magnetization (ΔM) between the field-cooled (FC) and the zero-field-cooled (ZFC) magnetization obtained from 10 K to 340 K did not converge to a zero value, indicating ferromagnetism above room temperature.

II. EXPERIMENT

Zinc oxide (0001) single crystals of 0.5 mm in thickness were prepared, and then 80 keV Fe ions with a dose of 3×10^{16} ions/cm² were implanted into the ZnO single crystals at 350 °C [10–12]. The projected range (Rp) of Fe ions was about 360 Å, and the maximum concentration near the Rp was about 8 atomic percent. The implanted samples were post-annealed at 700, 800 and 900 °C by rapid thermal annealing in a N₂ atmosphere for 5 min to re-crystallize the samples and to remove the ion-implantation damage.

The crystalline structure was investigated by using X-ray diffraction (XRD) with Cu-K α radiation. In order to extract information regarding the chemical states of the elements, X-ray photoelectron spectroscopy (XPS) was used with Al-K α radiation ($h\nu = 1486.6$ eV). The XPS spectra were calibrated to the C 1s photoelectron signal at 285 eV. The Magnetic properties of Fe-ion-implanted ZnO were investigated by using a superconducting quantum interference device (SQUID) magnetometer as a function of temperature and magnetic field. The magnetoresistance (MR) was measured with the Van der Pauw technique at various temperatures with the magnetic field parallel to the *c*-axis of the samples by using a magnetic property measurement system (MPMS).

III. CRYSTALLOGRAPHIC AND ELECTRONIC STRUCTURE

Crystallographic data are given below. These results show that Fe-ion-implanted ZnO has almost a hexagonal wurtzite ZnO structure. The XRD measurements were carried out on all samples annealed at 700, 800, and 900 °C, including as-implanted samples in the grazing mode using Cu-K α radiation at room temperature. Standard θ -2 θ scans were used to verify the hexagonal wurtzite structure.

Figure 1 shows representative XRD results for (a) as-implanted sample and (b) sample annealed at 900 °C. The XRD pattern shown in Figure 1 indicates that the films have a hexagonal wurtzite ZnO structure with a very small island peak (*) near 37°. This peak is a second phase peak and doesn't match with Fe compound like FeO, Fe₂O₃, and Fe₃O₄, even with the ZnFe compound, ZnFe₂O₄. The Fe or ZnFe compound doesn't have a peak near 37°. The peak does correspond to the (200) main reflection of cubic ZnO₂ [13]. The XRD graph was drawn again on logarithmic scale and was magnified to identify the small ZnO₂ peaks. The inset in Figure 1 shows the

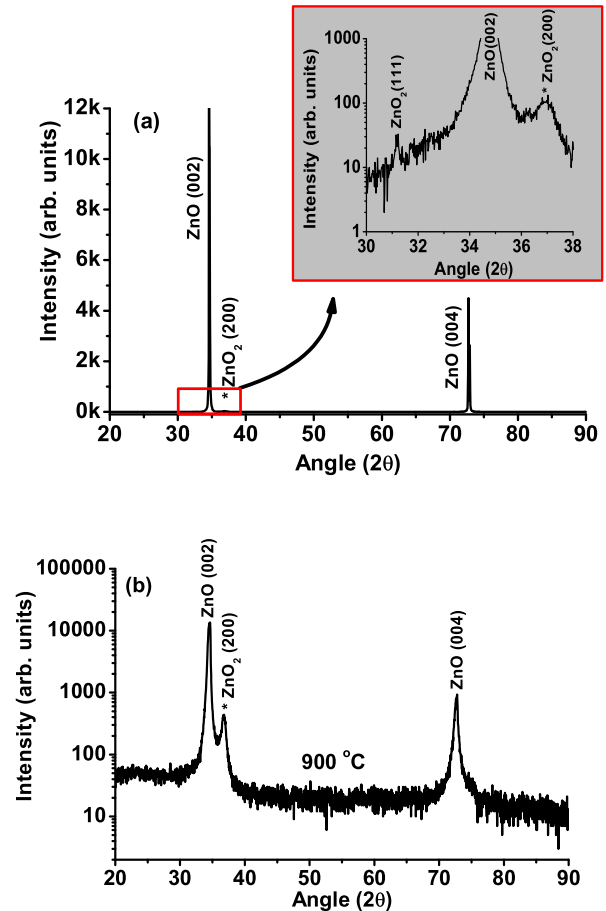


Fig. 1. X-ray diffraction data for (a) as-implanted samples and (b) samples annealed at 900 °C measured at room temperature. The graph shows a standard θ -2 θ XRD scan. The symbol * indicates a peak coming from ZnO₂ (200). The inset in Figure 1(a) shows the XRD intensity plotted on a logarithmic scale from 30 to 38°.

enlarged XRD graph in the range from $2\theta = 30$ to 38°. The main peak of ZnO₂ can be seen clearly, and there is another tiny peak between 31 and 32°. It is identified with a ZnO₂ (111), which is the second highest peak of ZnO₂. The ZnO₂ peak did not disappear after post-annealing at high temperature. As can be seen in Figure 1 (b) there are no second phases related with Fe, except for those ZnO₂ peaks, in all the films. The ZnO₂ peak seems to originate from Fe ions after ion implantation. The surplus oxygen could form ZnO₂ when Fe ions are substituted with oxygen during ion-implantation. The XRD rocking curve of annealed samples was measured at ZnO (002). The value of the full width at half maximum decreased from 0.24 to 0.17° with increasing the annealing temperature from 700 to 900 °C due to recovery of the crystal structure. The X-ray data provide evidence that the present Fe-ion-implanted ZnO films still have a hexagonal wurtzite ZnO structure, including a small

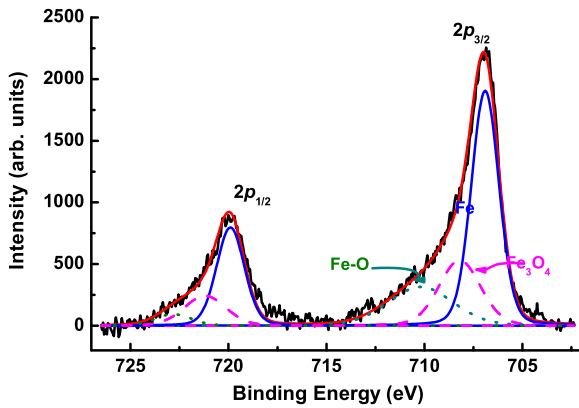


Fig. 2. XPS spectra of Fe 2*p* core levels. The first peak is Fe 2*p*_{1/2} at 720 eV, and the second peak is Fe 2*p*_{3/2} at 707 eV. The peaks were identified as Fe metal, FeO, and Fe₃O₄.

amount of ZnO₂.

XPS data were obtained in samples annealed at various temperatures. Figure 2 shows Fe 2*p* spectra for the sample annealed at 700 °C. Fe 2*p* core level spectra were convoluted with a Gaussian-Lorentzian function into three pairs of subpeaks, corresponding to Fe metal (Fe 2*p* = 706.9 eV), FeO (Fe 2*p* = 710.2 eV), and Fe₃O₄ (Fe 2*p* = 708.2 eV). The peaks indicate that the materials mainly included Fe metals. These Fe compositions could affect the magnetic properties because these materials have very high Curie temperatures compared to room temperature. Thus, we could expect the Curie temperature of all samples to be very high. The magnetization curves were measured for all samples to investigate the magnetic properties of Fe-implanted samples.

IV. MAGNETIC AND TRANSPORT PROPERTIES

The static magnetization *M* was measured as a function of a static externally applied field *H* and the temperature by using a SQUID produced by Quantum Design. The Data from all the samples were obtained in the plane applied field configuration. Figure 3 (a) shows the magnetization of the samples annealed at 700 °C as a function of the external magnetic field. The diamagnetic component was subtracted from the original data. The inset indicates low data, at 300 K without the diamagnetic component subtracted. It exhibits a conventional ferromagnetic hysteresis loop with a coercive force of about 458 Oe, saturation at an applied field of 800 Oe at 5 K, and with a coercive force of about 143 Oe, saturation at an applied field of 800 Oe at 300 K. The saturated magnetization *M*_s decreased from 7.5×10^{-5} to 4.5×10^{-5} emu with increasing temperature from 5 K to 300 K. The ferromagnetism was still there even at 300

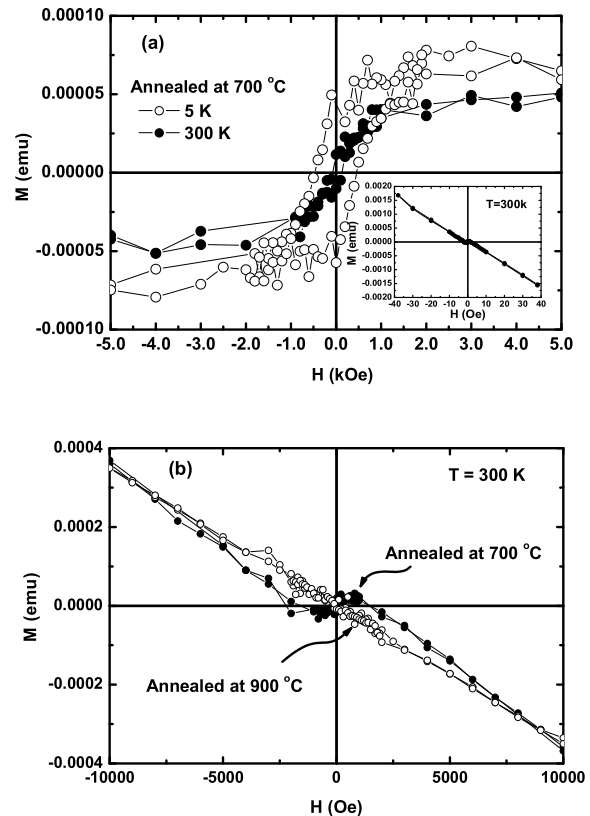


Fig. 3. (a) Ferromagnetic hysteresis loops of the samples annealed at 700 °C are shown for 5 and 300 K. The diamagnetic component was subtracted. The inset indicates low data, at 300 K without the diamagnetic component subtracted. (b) Ferromagnetic hysteresis loop of the samples annealed at 700 °C and diamagnetic loop of the samples annealed at 900 °C.

K. Figure 3 (b) shows the magnetization data measured at 300 K in the samples annealed at 700 °C and 900 °C to compare the magnetization in both samples, but the ferromagnetism at 300 K disappeared in the samples annealed at 900 °C. There is no hysteresis anymore, and only linear behaviors indicating diamagnetism are seen.

In order to observe the ferromagnetic state at temperature over 340 K, the temperature dependence of magnetization was taken in ZFC and FC. The 500 Oe magnetic field was applied in a plane during the measurement. Figure 4 show the magnetization data as a function of annealing temperature (a) 700 °C, (b) 800 °C, and (c) 900 °C. As can be seen in Figure 4 (a), the difference of magnetization ΔM between FC and ZFC did not converge to zero even at 340 K. The ferromagnetic state remains above 340 K, which is the limit of the SQUID magnetometer. However, the ΔM goes to zero at 270 K in Figure 4 (b). That is why the hysteresis loops aren't observed at 300 K in the samples annealed at 800 °C. With further increases in the annealing temperature, the magnetization goes to negative values in both the FC and the

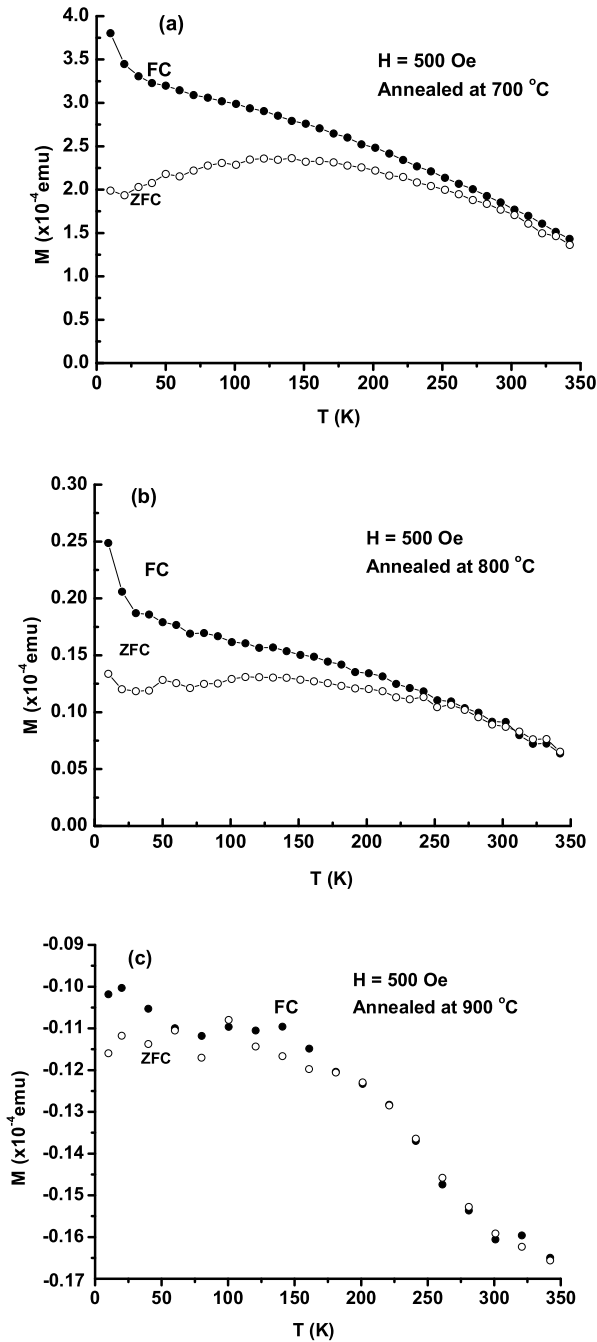


Fig. 4. Temperature dependences of FC and ZFC magnetizations for samples annealed at (a) 700 °C, (b) 800 °C, and (c) 900 °C.

ZFC measurement, indicating diamagnetism as in Figure 3 (b). Ferromagnetism isn't seen even in 5 K for a sample annealed at 900 °C. The ferromagnetic properties get weak with increasing annealing temperature. According to the XPS spectra, Fe metal was mainly included. If Fe metal contributes to the ferromagnetism, the Curie temperature should be very high because the Curie temperature of Fe metal is more than 1000 K. Therefore, the

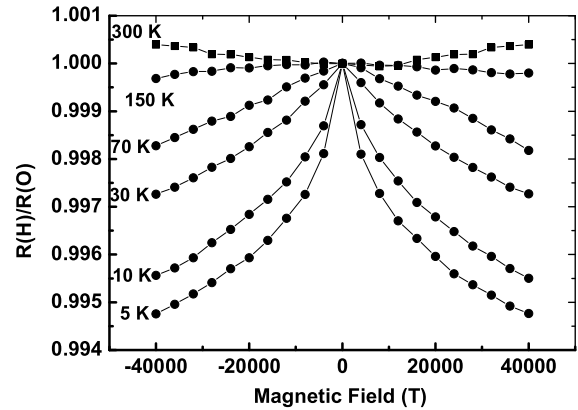


Fig. 5. Normalized magnetoresistance measured at various temperatures: 5, 10, 30, 70, 150, and 300 K. The applied magnetic field is parallel to the c -axis.

magnetic properties are not due to pure Fe metal even for the samples annealed at 700 °C. If both the electronic structure results and the magnetic data for the Fe-ion-implanted films are considered, the M_s values indicate that a fraction of Fe atoms are magnetically active, but that is not due to the Fe metal. The ferromagnetic state remains above 340 K in the samples annealed at 700 °C.

Isothermal MR was measured at various temperatures from 5 K to 300 K to study the s - d exchange interaction between the conducting s band electrons and the d electron spins localized at the Fe impurity in the Fe-ion-implanted samples. The magnetic field was applied parallel to the c -axis. Figure 5 shows normalized MR curves measured at various temperatures. One could obtain the MR curves to 300 K, and a negative curvature was seen in the temperature range from 5 K to 150 K. The MR data show a behavior similar to that reported by Jin *et al.* [14, 15] at this temperature range. It is known that the magnetotransport properties of magnetic semiconductor strongly depend on the charge carrier concentration [16, 17], which are electrons in intrinsically n -conducting ZnO. With decreasing electron concentration, at the metal-insulator transition, the character of the wave function changes from delocalized state to localized [18]. In the Fe-ion-implanted samples, the MR is negative, which can be explained with delocalized state due to the metallic behavior of ZnO implanted with Fe ions in the temperature range from 5 K to 300 K. The signal obtained at 300 K showed a positive curvature with a very weak signal. Considering the negative curvature from 5 K to 150 K, the positive curvature at this temperature cannot be understood at this time.

V. SUMMARY

Magnetic and transport properties of Fe-ion-implanted ZnO were investigated. All samples included very small

amounts of ZnO₂. Ferromagnetic properties were observed above room temperature for samples annealed at 700 °C. The MR curve showed negative curvature below 150 K, which is originated from delocalized *d* states of metallic ZnO.

ACKNOWLEDGMENTS

This work was supported by a Korean Science and Engineering Foundation grant (KOSEF-R01-2004-000-10882-0).

REFERENCES

- [1] S. D. Sarma, J. Fabian, X. Hu and I. Zutic, *IEEE Trans. Magn.* **36**, 2821 (2000).
- [2] H. Ohno, *Science* **281**, 951 (1998).
- [3] H. Ohno, D. Chibu, F. Matsukura, T. Omiya, E. Abe, T. Dietl, Y. Ohno and K. Ohtani, *Nature* **408**, 944 (2000).
- [4] Sato and H. Katayama-Yoshida, *Jpn. J. Appl. Phys.* **40**, L334 (2001).
- [5] H. Kim and C. H. Park, *J. Korean Phys. Soc.* **49**, 477 (2006).
- [6] T. Dietl, H. Ohno, F. Matsukura, J. Cibert and D. Ferrand, *Science* **287**, 1019 (2000).
- [7] K. Sato and H. Katayama-Yoshida, *Jpn. J. Appl. Phys.* **39**, L555 (2000).
- [8] A. F. Hebard, R. P. Rairigh, J. G. Kelly, S. J. Pearton, C. R. Abernathy, S. N. G. Chu and R. G. Wilson, *J. Phys. D: Appl. Phys.* **37**, 511 (2004).
- [9] W. Kim, H. J. Kang, S. K. Oh, Y. H. Cho, D. S. Yang, J. H. Lee, J. H. Song, S. K. Noh, S. J. Oh, C. S. Kim, S. W. Shin and C. N. Whang, *J. Korean Phys. Soc.* **49**, 979 (2006).
- [10] S. O. Kucheyev, P. N. K. Deenapanray, C. Jagadish, J. S. Willimas, M. Yano, K. Koike, S. Sasa, M. Inoue and K. Ogata, *Appl. Phys. Lett.* **81**, 3350 (2002).
- [11] S. O. Kucheyev, C. Jagadish, J. S. Williams, P. N. K. Deenapray, M. Yano, K. Koike, S. Sana, M. Inoue and K. Ogata, *J Appl. Phys.* **93**, 2972 (2003).
- [12] A. Y. Polyakova, A. V. Govorkova, N. B. Smirnova, N. V. Pashkova, S. J. Pearton, K. Ip, R. M. Frazier, C. R. Abernathy, D. P. Norton, J. M. Zavada and R. G. Wilson, *Materials Science in Semiconductor Processing* **7**, 77 (2004).
- [13] S Lindroos and M Leskela, *International. Inorganic Mat.* **2**, 197 (2000).
- [14] Z. W. Jin, K. Hasegawa, T. Fukumura, Y. Z. Yoo, T. Hasegawa, H. Koinuma and M. Kawasaki, *Physica E* **10**, 256 (2001).
- [15] S. S. Yan, C. Ren, X. Wang, Y. Xin, Z. X. Zhou, L. M. Mei, M. J. Ren, Y. X. Chen, Y. H. Liu and H. Garmestani, *Appl. Phys. Lett.* **84**, 2376 (2004).
- [16] T. Dietl, *Semimagnetic Semiconductors and Diluted Magnetic Semiconductors*, edited by M. Averous and M. Balkanski (Plenum Press, New York, 1991), p. 83.
- [17] J. K. Furdyna and J. Kossut, *Semiconductors and Semimetals*, Vol. 25, edited by R. K. Willardson and A. C. Beer (Academic Press, San Diego, 1988), p. 183.
- [18] Q. Xu, L. Hartmann, H. Schmidt, H. Hochmuth, M. Lorenz, R. Schmidt-Grund, C. Sturm, D. Spemann and M. Grundmann, *Phys. Rev. B* **73**, 205342 (2006).